Molecular Simulation
Vol. 38, Nos. 8–9, July–August 2012, 695–703

Bioinspired design of functionalised graphene

Zhao Qin[a,b] and Markus Buehler[a,b,c]*

[a]*Laboratory for Atomistic and Molecular Mechanics (LAMM), Department of Civil and Environmental Engineering, Massachusetts Institute of Technology, 77 Massachusetts Avenue, Cambridge, MA 02139, USA;* [b]*Center for Computational Engineering, Massachusetts Institute of Technology, 77 Massachusetts Avenue, Cambridge, MA 02139, USA;* [c]*Center for Materials Science and Engineering, Massachusetts Institute of Technology, 77 Massachusetts Avenue, Cambridge, MA 02139, USA*

(*Received 28 February 2012; final version received 11 April 2012*)

Functionalised graphene is an attractive candidate for novel applications in the fabrication of nanodevices or novel composites. Here, we apply molecular dynamics simulations to investigate the assembly of functionalised graphene ribbons and sheets. We illustrate that by designing the location and density of functional groups, the material self-assembles into a defined stable folded structure with lower energy and mechanical properties distinct from the pristine graphene. We show that the hydrogen bonds formed between the functional groups are crucial for this folding process, similar to the driving forces of assembly in many biological protein materials. We propose that such functionalised graphene materials could be employed to realise the bottom-up design of structural materials with tunable mechanical properties as they are expected to achieve multiple mechanical functions under varied conditions.

Keywords: graphene; bioinspired; functionalisation; simulation; hierarchical

1. Introduction

Graphene is a two-dimensional (2D) sheet of covalently bonded single layer of carbon atoms [1,2]. It forms the basis of graphite by stacking in thickness direction and carbon nanotubes by wrapping and fusing it along an axis. Recent experimental advances in synthesis, characterisation and manipulation of graphene have resulted in very significant interest in this material because of its outstanding mechanical, thermal and electronic properties [3–5]. Its intrinsic strength, predicted to exceed than that of any other material, motivates its wide engineering applications in a wide range of industries including space technology, automotive development or civil engineering [5]. For example, it has been proposed to be used as the reinforcement for polymer nanocomposites, which may allow us to build a space elevator if the strength of the macroscopic fibre can reach its theoretical limit of graphene ribbons at the nanoscale.

Several approaches, including chemical methods and mechanical methods, were developed and applied to obtain individual graphene sheets or flakes [6–8]. Chemical methods can produce graphene in large quantity but inevitably leave chemical groups attached to the graphene during the production. In addition, these chemical groups can enhance the adhesion of graphene with the polymers in the composite by adding interactions among the functional groups and can facilitate in forming paper-like composite materials [9–11]. However, it remains elusive how the graphene conformation and resulting material properties can be controlled by the distribution of functional groups, which prevents us from exploiting their full potential in the bottom-up fabrication of materials with designed morphology and material characteristics.

Apart from mechanical enhancement, functional groups can alter the molecular conformation of graphene. Proper designs of the amount and location of functional groups combined with altering the geometry of graphene sheets may enable us to fabricate materials with certain conformations and functions. The idea we propose here is to use graphene as a backbone, and to exploit functional groups as side chains is analogy to the protein folding processes [12,13], through which peptide backbones manage to reach various folded structures and various mechanical properties because of the existence of different interactions among 20 different types of side chains. This hypothesis makes graphene an attractive candidate in bottom-up design materials with tunable mechanical properties [14,15].

In this study, we elucidate atomic structures and mechanical properties of the folded functionalised graphene based on molecular dynamics simulations using the combination of the Adaptive Intermolecular Reactive Empirical Bond Order (AIREBO) Potential [16,17] and Chemistry at HARvard Molecular Mechanics (CHARMM) force field [18]. In this study, we use hydroxyl groups as functional units attached to the graphene surface because this chemical group can play both the roles of a donor and an acceptor in forming hydrogen bonds. We find that the network of hydrogen bonds formed among the functional groups plays an important role in governing the

*Corresponding author. Email: mbuehler@mit.edu

ISSN 0892-7022 print/ISSN 1029-0435 online

http://dx.doi.org/10.1080/08927022.2012.685943
http://www.tandfonline.com

conformations and mechanical properties of the graphene. Functionalised graphene changes its morphology to adapt the conformation with lowest energy, and our results suggest that by the rational design of the atomic structure of the functionalised graphene, the manufacturing of a series of materials with uniform chemical composition as well as diverse material properties can be achieved.

2. Molecular modelling methods

We use a hybrid force field to model the functionalised graphene here. The internal interactions among carbon atoms in the graphene are described by the AIREBO force field [16], whereas the interactions among the hydroxyl functional groups are described by CHARMM force field [18]. The total potential energy of the system is composed of the bonding energy, angular energy and pair energy as:

$$E = \sum E_{\text{bond}} + \sum E_{\text{angle}} + \sum E_{\text{pair}}. \tag{1}$$

Each energy term is given by $E_{\text{bond}} = K_{ij}(r - r_0)^2$, $E_{\text{angle}} = K_{ijk}(\theta - \theta_0)^2$, and $E_{\text{pair}} = E_{\text{CH}} + E_{ij}$, where r_0 is the bond length at equilibrium, θ_0 is the angle at equilibrium, K_{ij} and K_{ijk} are the stiffness of the bond and angle, respectively. The E_{CH} term of the pair potential refers to the short-range interactions among carbon atoms and hydrogen atoms connected directly to carbon atoms and the E_{ij} term refers to the long-range interaction among all types of atoms. These two terms are of the expression as

$$E_{\text{CH}} = \frac{1}{2}\Sigma_i\Sigma_{j\neq i}\left[E_{ij}^{\text{REBO}} + \Sigma_{k\neq i}\Sigma_{l\neq i,j,k}E_{kijl}^{\text{TORSION}}\right] \tag{2}$$

$$E_{ij} = \Sigma_i\Sigma_{j\neq i}\left\{4\epsilon\left[\left(\frac{\sigma}{r_{ij}}\right)^{12} - \left(\frac{\sigma}{r_{ij}}\right)^{6}\right] + \frac{c_{q_iq_j}}{r_{ij}}\right\} \tag{3}$$

where E_{ij}^{REBO} denotes the reactive empirical bond order (REBO) term of hydrocarbon [17] and $E_{kijl}^{\text{TORSION}}$ is an explicit 4-body potential that describes various dihedral angle preferences in hydrocarbon configurations. The detail expression and parameters of E_{ij}^{REBO} and $E_{kijl}^{\text{TORSION}}$ are given in the original paper of this force filed [16]. In the E_{ij} term, ϵ is the interacting energy, σ is the zero energy distance, C is the energy-conversion constant, q is the charge relative to the electron charge and r_{ij} is the distance between atom i and j. The values of these parameters applied in our model are as summarised in Table 1.

We model the structure of the 2D graphene by placing carbon atoms in a standard hexagonal lattice with a lattice constant of $a = 1.42$ Å. The resulting structures have zigzag chirality in one direction and armchair chirality in the other (orthogonal) direction, as shown in Figure 1(a). Hydroxyl groups are adopted as functional groups in this study as have been employed in the former studies. These functional groups are randomly attached on both sides of the graphene surface as depicted in Figure 1(a). The concentration of the functional groups is defined by $C = N_{\text{func}}/N_{\text{C}}$, where N_{C} is the total number of carbon atoms and N_{func} is the total number of the functional groups. The width of the graphene is W in one direction and the length is L in the orthogonal direction. The open edges of the graphene are terminated covalently with hydrogen atoms. We can directly obtain the relationship between the geometry and the amount of carbon atoms as $N_C = 4WL/(3\sqrt{3}a^2)$.

Table 1. The value of the parameters applied in molecular dynamics simulations in this study [16,18].

Parameter and units	Numerical value
Harmonic bond stiffness K_{OC} (kcal/mol/Å^2)	334.3
Harmonic bond stiffness K_{OH} (kcal/mol/Å^2)	545.0
Equilibrium distance r_{0_OC} (Å)	1.411
Equilibrium distance r_{0_OH} (Å)	0.96
Harmonic angle stiffness K_{COH} (kcal/mol)	65
Equilibrium angle θ_{0_COH} (°)	108
Zero-potential distance σ_{C} (Å)*	3.4
Zero-potential distance σ_{O} (Å)*	3.15
Zero-potential distance σ_{H} (Å)*	0.4
Minimum energy ϵ_{C} (kcal/mol)*	0.07
Minimum energy ϵ_{O} (kcal/mol)*	0.1521
Minimum energy ϵ_{H} (kcal/mol)*	0.0460
Electrostatic constant C (Åkcal/mol)	332.1
Charge relative to the electron charge q_{C} (in pristine graphene, sp2-hybridised)	0.0
Charge relative to the electron charge q_{C} (in triplet of COH, sp3-hybridised)	0.11
Charge relative to the electron charge q_{O}	−0.54
Charge relative to the electron charge q_{H}	0.43

*The LJ potential between any atom pair follows the arithmetic mixing rule as $\epsilon_{ij} = \sqrt{\epsilon_i\epsilon_j}$ and $\sigma_{ij} = (\sigma_i + \sigma_j)/2$.

3. Results and discussion

The equilibrated conformation of a single graphene sheet is largely affected by the concentration of the functional groups as is expressed by the fluctuation of the carbon atoms in the normal direction of the sheet, as shown in Figure 1(b). We find the hydrogen bonds that form among the functional groups account for this fluctuating geometry as shown in Figure 1(a). A hydrogen bond can only form on one side of the graphene sheet and thereby induces the protrusion as it locates at the top surface and induces a dent as it locates at back surface. The mixture of dents and protrusions in the graphene sheet is illustrated by different colours as shown in Figure 1(b), and the characteristic wavelength is given by λ. We change the concentration of the functional group and find that the wavelength decreases as C increases as visualised in Figure 1(c). It is caused by the fact that the increasing C increases the probability to form hydrogen bonds on both sides of the

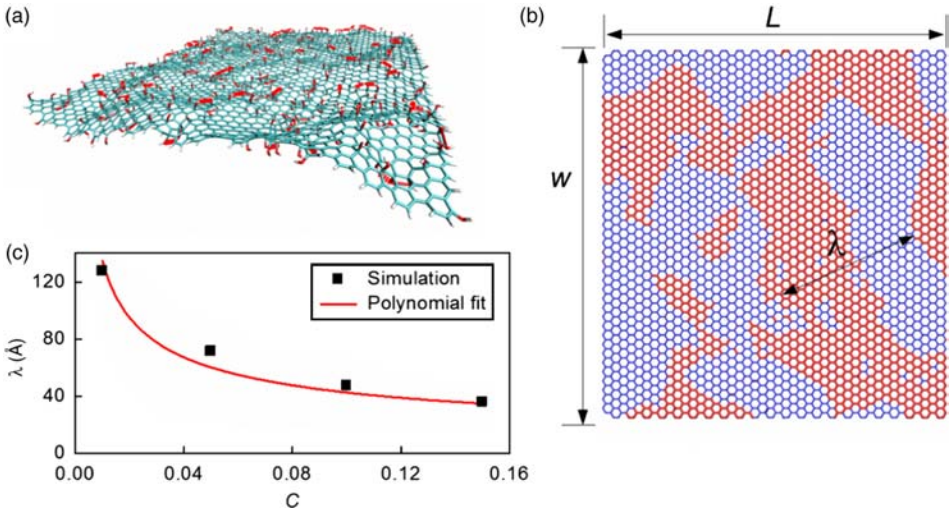

Figure 1. The conformation of a graphene sheet functionalised by hydroxyl groups, in equilibrium. (a): The snapshot of a functionalised graphene sheet in equilibrium with the size of 100 Å × 100 Å, where the concentration of functional groups is $C = 10\%$ with a random distribution. The carbon atoms are in cyan, oxygen atoms are in red and hydrogen atoms are plotted in white. Hydrogen bonds are depicted by red dashed lines. (b): The fluctuation of the carbon atoms in the normal direction of the sheet; atoms with positive displacement are shown in red and atoms with negative displacement in blue. The characteristic wavelength is measured from snapshots of the equilibrated graphene sheets and denoted by λ. (c): The characteristic wavelength as a function of the concentration of the functional groups. The polynomial fit is $\lambda = 13.46/\sqrt{C}$.

graphene, and thus decrease the average area of each hydrogen, as well as the characteristic length λ. By applying this analysis, we can fit the result to the scaling law $\lambda \sim 1/\sqrt{C}$. As shown in the plot, the fitted curve agrees rather well with the simulation result.

This result that the density of functional groups controls the fluctuations of the graphene sheet is interesting since it affects the modulus of the material. More fluctuations imply a decreasing modulus of graphene because greater deformation is needed initially to fully align the graphene sheet in plane before deforming the graphene and its stiff carbon–carbon bonds directly. In our simulations, the modulus of graphene decreases from 0.8 TPa (taking the thickness as $t = 3.4$ Å) for pristine graphene to 0.6 TPa for functionalised graphene with $C = 15\%$. This result agrees with earlier computational studies using a different force field (1.05 TPa for the pristine graphene and 0.70 TPa for 15% functionalised graphene [19]).

The reason to use the combined force field is that the original AIREBO force field gives correct energies of pure hydrocarbon systems, but does not contain parameters for hydroxyl groups [17]. Some recent work overcoming this limitation has extended the AIREBO force field to include hydroxyl groups (by considering bonded interactions). However, the (non-bonded) hydrogen bond interactions in that model were not fully validated [20]. Since the hydrogen bonding energy (~6.2 kcal/mol for our model) is much smaller than the covalent bond (~43 kcal/mol for the C–O bond), the rupture and reforming of the hydrogen bond dominates the material behaviour, and as such is a critical model property. The established CHARMM force field gives a widely validated description of the hydrogen bonding interaction. Moreover, the hydrogen bonding energy given by our model agrees to that given by the first-principles based ReaxFF force field, leading to a value of ~7.4 kcal/mol [9]. It is noted that one limitation of our model is that it does not include the functional-group effect on the C–C bond strength. The model may also lack some accuracy at the ultimate strength of the graphene. However, away from such extreme conditions, the mechanical properties match the existing results rather well (e.g. the modulus, as discussed above).

To investigate how significant conformational changes can be caused by the functional groups, we focus on an extreme case of a graphene ribbon with a size of 5 Å × 500 Å. Two graphene ribbons, one being pristine graphene and the other one being functionalised graphene with $C = 15\%$ are carefully compared as shown in Figure 2(a). Both ribbons start as a straight conformation. It is observed that the functionalised graphene ribbon reaches a folded state quite rapidly as the simulation starts, whereas the pristine graphene ribbon does not reach any folded state but fluctuates as an unfolded hairpin as shown in Figure 2(b). The total potential energy decreases by ~1200 kcal/mol for the folded state of the functionalised graphene ribbon. Most of the energy comes from the interaction of among functional groups, and that explains why the pristine graphene ribbon does not fold with into an energy favoured conformation.

We investigate the mechanical property of the random folded structure of the graphene ribbon with randomly attached functional groups by applying tensile force in

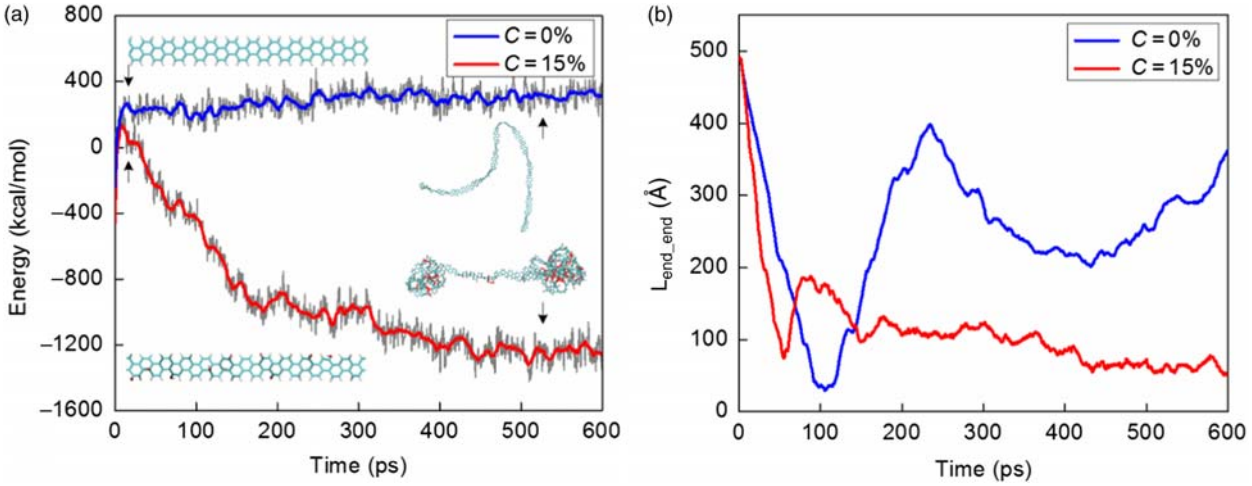

Figure 2. The comparison of the folding of the graphene ribbons with the size of 5 Å × 500 Å under the temperature of 300 K. (a) The energy histories of the folding process of two graphene ribbons, one is pristine and the other is functionalised by 15% hydroxyl groups with random distribution. The functionalised graphene ribbon starts with a straight conformation (partly shown by the inserted picture at left bottom corner) and reaches a folded structure composed of two globular folds after ~500 ps calculation. The pristine graphene ribbon starts as a straight conformation (partly shown by the inserted picture at left-up corner) and does not reach the folded conformation in the simulations. Moving averages of the curves are taken with a window of 10 ps. (b) The end-to-end distance of the pristine and functionalised graphene ribbons during the simulation. For pristine graphene, its conformation keeps changing in time while for functionalised graphene its structure reaches a relatively stable state after folding.

steered molecular dynamics (SMD) simulations. The tensile force applied to the two ends of the folded structure makes it unfold as shown in Figure 3(a). The force first increases as the extension increases before reaching a first plateau at ~38 Å as shown in Figure 3(b), and the folded structure remains intact as the hydrogen bond number stays at a relative constant value before reaching a plateau as shown in Figure 3(c). For the plateau region, the folded structure starts to unfold by breaking the hydrogen bonds among functional groups as illustrated in Figure 3(a). The tensile force becomes 'bumpy' in this region and the hydrogen bond number decreases continuously. The graphene ribbon is fully unfolded once all hydrogen bonds break and the ribbon itself gets deformed as the end-to-end distance approaches the contour length. Then, the force increases significantly until reaching the breaking point of the ribbon as shown in Figure 3(b). This force–extension curve is similar to what has been observed in the unfolding process of coiled protein materials

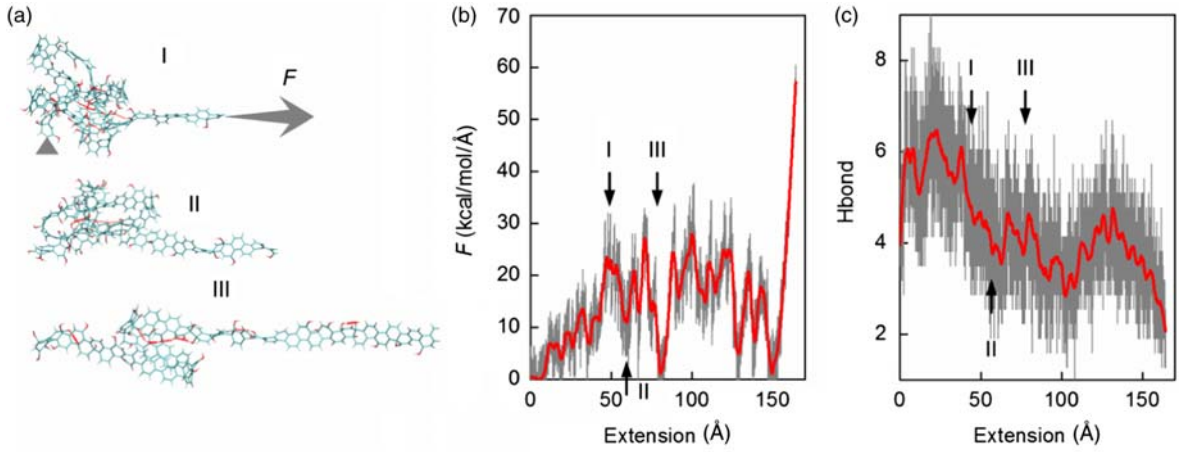

Figure 3. (Colour online) The unfolding of a folded functionalised graphene ribbon. (a) A globular folded structure of the functionalised graphene ribbon (folding process shown in Figure 2) is loaded by a tensile force that is applied at the end of the ribbon with a relative displacement rate of 0.1 Å/ps, using SMD. The snapshots are taken at extensions of 48 Å, 60 Å and 73 Å. (b) The force–extension curve as recorded during the unfolding process of the folded graphene ribbon. (c) The number of hydrogen bonds as a function of the extension as is recorded during the unfolding process. The red curves in (b) and (c) are moving averages with a window of 10 ps.

[21–23], providing some evidence that they share similar mechanism in forming the folded structure.

We investigate the persistence length of the functionalised graphene ribbon by studying trajectories for each model in the simulation. We examine three segments with the length of $s-s' = 42.6$ Å (where s and s' are coordinates along the contour lengths of the chain) and assess the time average of the angles between the directions of the ends of the segments as $< \vec{t(s)} \cdot \vec{t(s')} >$. The results are as summarised in Table 2. Using the definition of the persistence length L_p as

$$< \vec{t(s)} \cdot \vec{t(s')} >= \exp\left[-\frac{s-s'}{L_{\mathrm{p}}}\right]. \quad (4)$$

We compute the persistence length of the graphene ribbon as summarised in Table 2. The pristine graphene ribbon is found to be $L_{\mathrm{p}} = 122.92 \pm 11.22$ Å at 300 K, whereas for all the other functionalised cases the graphene gets into a folded structure under the same temperature, this value agrees to former study of the persistence length of pristine graphene ribbons [24]. For a higher temperature of 1000 K, the pristine graphene ribbon features a decreased persistence length as $L_{\mathrm{p}} = 86.56 \pm 37.62$ Å and functional groups decrease this number to $L_{\mathrm{p}} = 54.41 \pm 27.01$ Å for $C = 5\%$. For $C = 15\%$, even the high temperature of 1000 K cannot prevent the ribbon from self-folding. The persistence length of this graphene ribbon is an order of magnitude larger than the persistence length of the protein backbone [25] (~12 Å) while smaller than that of DNA [26] (~500 Å). Since both of these biological materials can reach various folded structures by non-bonded interactions, we are inspired to design folded structures based on graphene ribbons, as an analogy to protein and DNA folding. It is noted that the calculation result at such high temperature (1000 K) may only have qualitative meaning for comparison because molecular modelling can loose its accuracy as the chemical desorption of hydroxyl groups occurs at this high temperature [27].

To develop some initial understanding of functionalised graphene ribbons' potential to form specific folded structures at room temperature, we focus on a simple case by putting two functional groups to the mid region of the graphene ribbon, and identifying its conformation at equilibrium. Two possible configurations of the functional groups exist: one for the two functional groups at different sides of the ribbon and the other for the two functional groups at the same side of the ribbon, as shown in Figure 4(a). We find for the first configuration, the graphene ribbon acts in the similar way as in the pristine case: it fluctuates through the simulation as shown by its end-to-end distance but never reaches folded conformations with favoured energy as shown in Figure 4(a), (b). For the second configuration, the two same-side hydroxyl groups form a single hydrogen bond between them and this interaction manages to act as a clamp to fold the graphene ribbon into two halves, as shown in Figure 4(c). It is quite interesting to see that the two halves coil with each other to form the double-helix structure along the same axis after only 58 ps of simulation time. The rising of each loop along the axis is measured to be ~57 Å, the diameter as ~7 Å and the persistence length of this structure is ~536.37 Å, which is more than four times than that of the pristine graphene ribbon, and similar to that of DNA molecules. The total potential energy of this double-helix structure is less (of 250 kcal/mol as shown in Figure 4(a)) than that of the unfolded case and its conformation is quite stable in our simulations as shown by the converged end-to-end length given in Figure 4(b).

Table 2. The persistence length of the graphene ribbon with various concentrations of functional groups and two temperature conditions (300 and 1000 K) in simulations.

C	$< \vec{t(s)} \cdot \vec{t(s')} >$	$(s\text{-}s')$ (Å)	$< L_{\mathrm{p}} >$ (Å)
0 (300 K)	0.72255	42.6	122.92 ± 11.22
	0.67922		
	0.71604		
1% (300 K)	Self-folded		
5% (300 K)	Self-folded		
15% (300 K)	Self-folded		
Double helix	0.84932	87.6	536.37
0 (1000 K)	0.45023	42.6	86.56 ± 37.62
	0.71585		
	0.58265		
1% (1000 K)	0.47821	42.6	85.75 ± 25.98
	0.67664		
	0.62434		
5% (1000 K)	0.19443	42.6	54.41 ± 27.01
	0.47628		
	0.58628		
15% (1000 K)	Self folded		

We have run the simulation several times to account different random velocity distributions at the beginning, and the formation of the double-helix structure is repeatable. We have also changed the relative distance of the two hydroxyl groups from 2.5 to 3.8 Å and found that as long as the two hydroxyl groups are to the one side of the ribbon (or they can cross the energy barrier to shift to one side of the ribbon) and are able to form a hydrogen bond between, the same double-helix conformation is reached. The folded graphene morphology as a hairpin is driven by the vdW interactions within the graphene ribbon. The key cause to make this morphology different from that of a pristine graphene ribbon, which tends to form scrolls, is a single hydrogen bond formed between the two hydroxyl groups at the middle of the graphene ribbon. This specific morphology as observed here is initially induced by geometry change in the graphene ribbon to form a kink to facilitate the self-folding. Here, we have shown that two functional groups and a single hydrogen bond can significantly affect the folded confor-

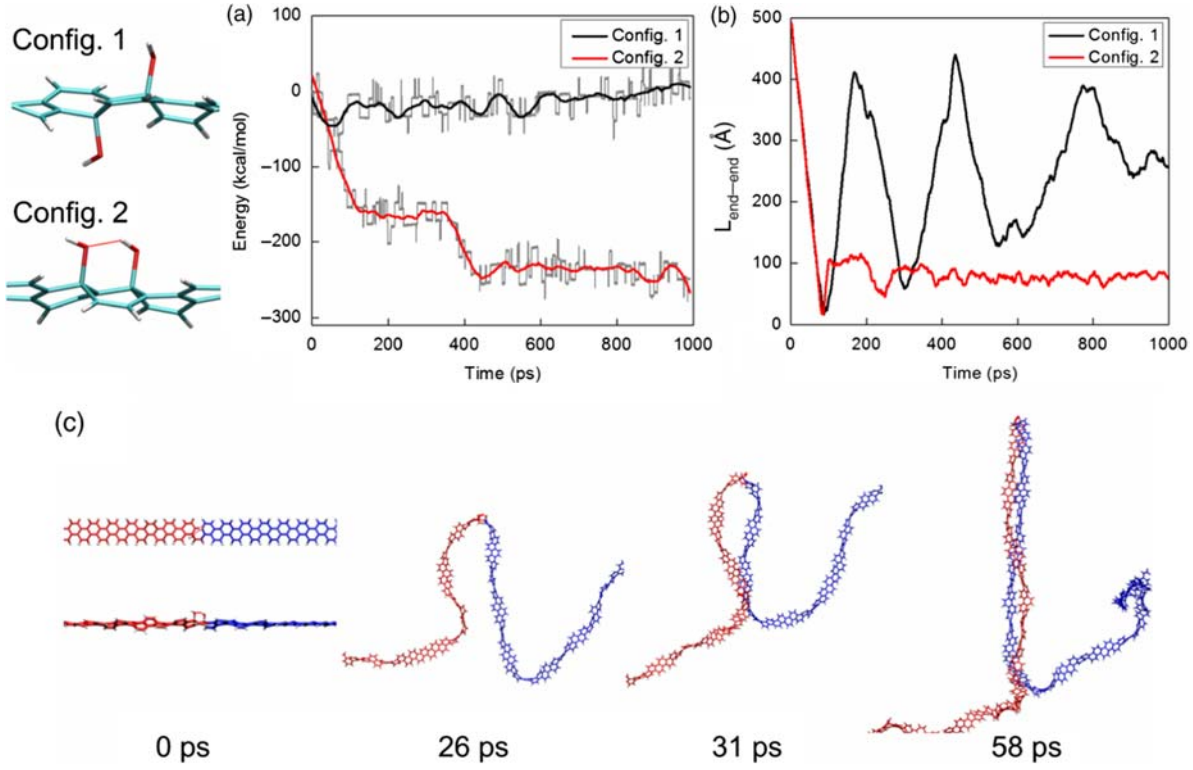

Figure 4. (Colour online) A coiled structure of the graphene ribbon formed by using two distinct functional groups. (a): Graphene ribbons with two functional groups, one at two different sides of the ribbon and another with functional groups at the same side of the ribbon. Both are equilibrated for comparison. The energy of the second graphene ribbon decreases in equilibrium whereas the first graphene ribbon does not have energy favoured state. The continuous curves are moving averages with a window of 100 ps. (b): The end-to-end distance of the graphene ribbons with different set-ups of the functional groups. The first one keeps fluctuating through the calculation whereas the second one reaches a folded state in a short time. (c): Simulation snapshots of the folding process of the graphene ribbon with the second set-up of the functional groups at 0 ps (up: top view; below: side view), 26 ps, 31 ps and 58 ps. The graphene ribbons to the left of the functional groups and to the right of the functional groups are in different colours for clarity. The continuous self-folded coiled structure with a rising of 57 Å along the axis for each loop is formed as shown after 58 ps calculation.

mation of a uniform graphene ribbon, leading to a stable double-helix morphology with a much larger persistence length. More complex geometries of the graphene ribbon itself and controlling the distribution of the functional groups may lead to other folded conformations with potentially distinct structural, electronic or mechanical properties and are yet to be discovered.

For biological materials, the interfacial properties among different domains are crucial in defining the materials properties. For example, the length of beta strands plays an important role in defining the shearing strength of beta crystals because it is governed by the cooperative deformation of hydrogen bonds [21–28,29], an important issue in silk or amyloid materials. It is natural to ask how the size of functionalised graphene accounts from its interfacial strength. We answer the question by setting up a double-layer graphene system with $C = 15\%$ and carry out shearing and tearing tests as shown in Figure 5(a),(c), respectively. For the shearing test, one edge of the bottom graphene sheet is fixed by removing the velocity of a single layer of the atoms at the edge, whereas the other edge of the top graphene sheet is under quasi-static tensile loading in the direction along the plane. For the tearing test, the bottom graphene sheet is fixed and the quasi-static loading is applied to the top graphene sheet at the edge. We keep a record of the tensile force as a function of the extension as shown in Figure 5(b). We change the size of the overlapped region from 20 Å × 20 Å to 180 Å × 180 Å by changing the geometry of the top graphene layer, and three force–extension curves are as shown. For the shearing case, it is observed that a linear region is found before reaching the peak shearing force and thereafter the force level begins to drop linearly as the contact area decreases. For the tearing test, the force slowly increases to a peak value as shown in Figure 5(d) because of the existence of the boundary with 20 Å in length that is free from attachment. For both the tests, we find that the peak force simply increases as the contact area increases. For the beta sheet crystals in spider silk, there exists an optimal length beyond which the shearing strength does not increase anymore. However, for the current functionalised graphene system we do not find a converged peak shearing

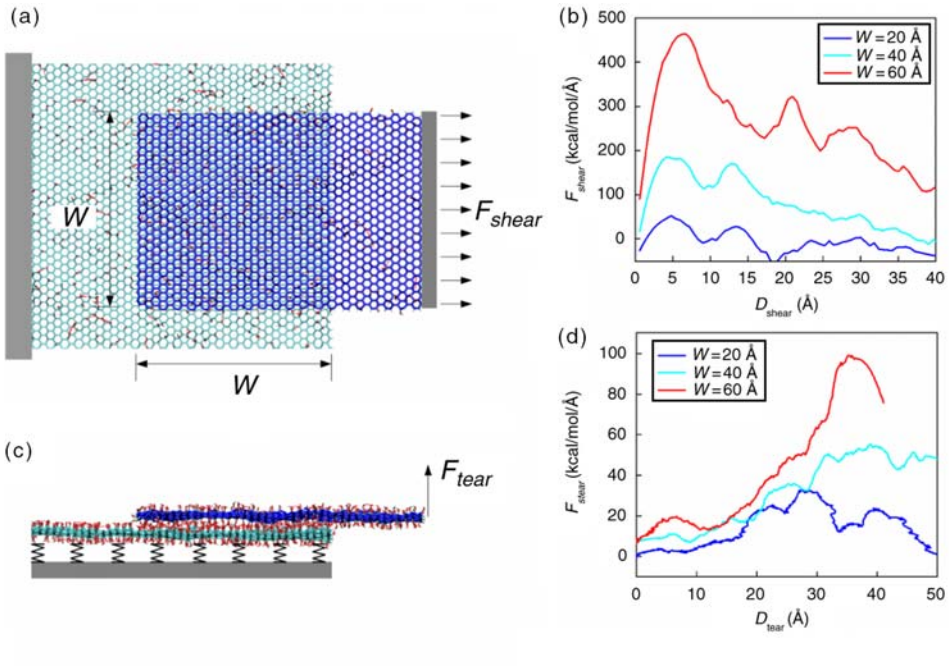

Figure 5. (Colour online) Shearing and tearing tests of the mechanical properties of functionalised graphene sheets in adhesion. (a) The top view of the set-up of the shearing test. Two graphene sheet with the concentration of functional groups as $C = 15\%$ with random distribution are in contact with a square area of $W \times W$. One edge of the bottom graphene sheet is fixed by removing the velocity of a single layer of the atoms at the edge, whereas the other edge of the top graphene sheet is under quasi-static tensile loading. (b) The force–extension relationships for systems under shearing loads with different contact graphene lengths. The increasing length leads to a larger peak force before sliding apart. (c) The side view of the set-up of the tearing test. The bottom graphene sheet is fixed by springs (stiffness constant as 20 kcal/mol/Å^2) tethered to each carbon atom and the quasi-static loading is applied to the top graphene sheet at the edge. (d) The force–extension relationships for systems under tearing loads with different contact graphene lengths. The increasing length leads to a larger peak force before tearing apart.

force up to $W = 180$ Å in our simulations. This is because the 2D graphene sheet provides a matrix confinement around the functional groups that are much more stiffer than the 1D peptide backbone [29], leading to a more uniform deformation of all the hydrogen bonds as the force applied. This analysis is supported by the observation in all our simulations that the displacements of every carbon atom along the shearing direction are uniform.

We summarise the shearing strength and tearing strength of the adhesion of the functionalised graphene sheets as functions of the sheet length as shown in Figure 6(a). It is observed that the shearing strength increases proportional to the surface area of the contacting region with a function of $F_{\text{shear\_max}} = C_{\text{shear}} W^2$, with $C_{\text{shear}} = 0.0931$ kcal/mol/Å^3, while the tearing strength increases proportional to the edge length of the contacting region with a function of $F_{\text{tear\_max}} = C_{\text{tear}} W$, with $C_{\text{tear}} = 1.439$ kcal/mol/Å^2. It is because the graphene is so thin that the bending stiffness is orders of magnitudes smaller than the tensile stiffness, and thereby in contrast to the shearing load that all the hydrogen bonds contributes to generate the friction force, the tearing load only lead to the concentrated deformation of hydrogen bonds within a short range along the edge. This property could be applied in fabricating removable coating materials as shown in Figure 6(b). Small pieces of the functionalised graphene could be used to coat the surface of metal, plastic, glass or other engineering materials. The high strength characteristic of graphene sheet ensures the endurance of the coating, the single-atom thickness accounts for its transparency, the functional groups account for strong adhesion force in shearing and the finite size of the sheets overcomes the complex curvature at the surface of micro devices such as atomic force microscopy (AFM) tips.

4. Conclusion

In this study, we investigated the assembling, structure and mechanical properties of functionalised graphene materials. It is found that functional groups attached to a graphene surface can significantly affect its conformation by forming hydrogen bonds among these groups. With proper design of the amount and location of functional groups, folded structures with lower energies can be reached. Especially, a single hydrogen bond formed by two functional groups can trigger an interesting self-folding mechanism in which a graphene ribbon transforms into a double-helix form with a much larger persistence length (and changed mechanical properties). Folded

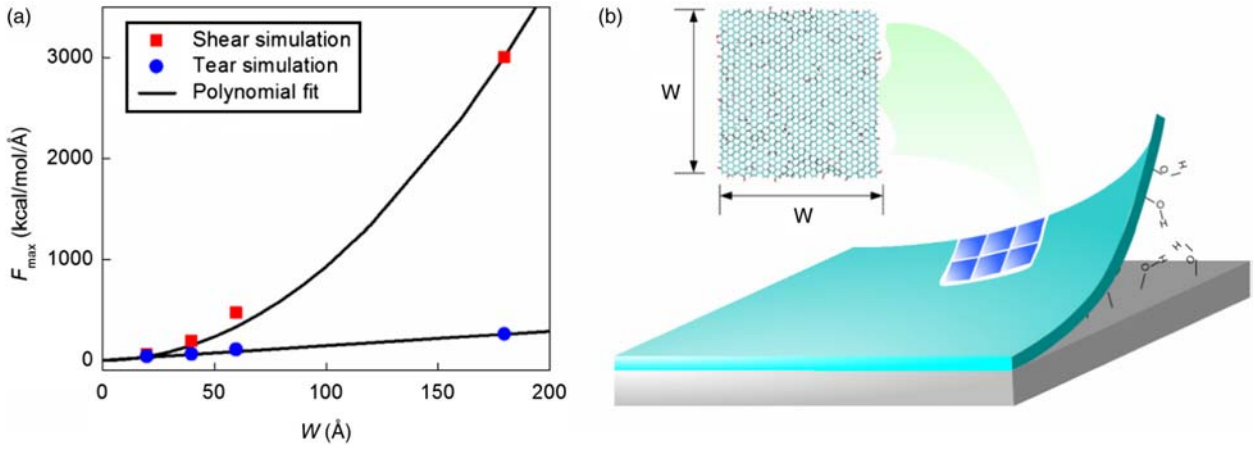

Figure 6. (Colour online) The size of the function graphene sheet is important in controlling the shearing and tearing strength of the material. (a): Simulation results of peak shearing forces and tearing forces before breaking apart of the graphene sheets, plotted as a function of the graphene length in contact. The shearing force is proportional to the contact area whereas the tearing force is proportional to the edge length as shown by different polynomial fitted curves. (b): Proposed set-up of a micro device coating method by using functionalised graphene sheets.

graphene structures are stable and have the unfolding curves similar to what is known from biological protein molecules. We also studied the adhesion strength of the functionalised graphene interface and found that it is a monotonic function of the contacting length, which ensures its potential as a potent coating material.

It is noted that all the simulations in this study are based on the model of graphene functionalised by pure hydroxyl groups. This single functional group simplifies the modelling and design process because it can be both a donor and an acceptor in forming hydrogen bonds. There are other external factors, for example, the existence of the defects and dislocations within graphene or other functional groups like epoxy or carboxyl groups, which can affect the result. Further molecular dynamics simulations for much larger systems are needed to include those factors into the model, and to investigate the material morphology and mechanical properties.

Various protein materials have a universal backbone but have significant different mechanical properties [15]. For example, intermediate filament proteins are extensible and flexible at small strain, whereas spider silk proteins are less stretchable but feature a much higher strength. These mechanical characteristics are due to the fact that each material is encoded by chains of amino acids with different sequences made up from 20 different types of side chains that diversify interactions among amino acids, leading to various hierarchical conformations [30]. Graphene, as a low-dimensional material with a perfect lattice structure and extreme strength, is perfect to be used as the building block to form materials with great diversity, in analogy to protein materials. The molecular structure of the graphene, including its geometry, chemical property and location of the functional groups, is important in affecting the morphology and material property of the structure, while the computational simulation show a significant advantage in facilitating this design work. By means of quantitative calculation and combining with experimental efforts, it may be possible to design and produce the next generation graphene-based materials.

Acknowledgements

This work was supported primarily by AFOSR.

References

[1] A.K. Geim and K.S. Novoselov, *The rise of graphene*, Nat. Mater. 6 (2007), pp. 183–191.
[2] J.C. Meyer, A.K. Geim, M.I. Katsnelson, K.S. Novoselov, T.J. Booth, and S. Roth, *The structure of suspended graphene sheets*, Nature 446 (2007), pp. 60–63.
[3] A.H. Castro Neto, F. Guinea, N.M.R. Peres, K.S. Novoselov, and A.K. Geim, *The electronic properties of graphene*, Rev. Mod. Phys. 81 (2009), pp. 109–162.
[4] A.A. Balandin, S. Ghosh, W.Z. Bao, I. Calizo, D. Teweldebrhan, F. Miao, and C.N. Lau, *Superior thermal conductivity of single-layer graphene*, Nano Lett. 8 (2008), pp. 902–907.
[5] C. Lee, X.D. Wei, J.W. Kysar, and J. Hone, *Measurement of the elastic properties and intrinsic strength of monolayer graphene*, Science 321 (2008), pp. 385–388.
[6] A.K. Geim and P. Kim, *Carbon wonderland*, Sci. Am. 298 (2008), pp. 90–97.
[7] S. Bae, H. Kim, Y. Lee, X.F. Xu, J.S. Park, Y. Zheng, J. Balakrishnan, T. Lei, H.R. Kim, Y.I. Song, Y.J. Kim, K.S. Kim, B. Ozyilmaz, J.H. Ahn, B.H. Hong, and S. Iijima, *Roll-to-roll production of 30-inch graphene films for transparent electrodes*, Nat. Nanotech. 5 (2010), pp. 574–578.
[8] D. Sen, K.S. Novoselov, P.M. Reis, and M.J. Buehler, *Tearing graphene sheets from adhesive substrates produces tapered nanoribbons*, Small 6 (2010), pp. 1108–1116.
[9] N.V. Medhekar, A. Ramasubramaniam, R.S. Ruoff, and V.B. Shenoy, *Hydrogen bond networks in graphene oxide composite paper: Structure and mechanical properties*, ACS Nano 4 (2010), pp. 2300–2306.
[10] D.R. Paul, *Creating new types of carbon-based membranes*, Science 335 (2012), pp. 413–414.

[11] R.R. Nair, H.A. Wu, P.N. Jayaram, I.V. Grigorieva, and A.K. Geim, *Unimpeded permeation of water through helium-leak-tight graphene-based membranes*, Science 335 (2012), pp. 442–444.
[12] A.V. Finkelstein, O.V. Galzitskaya, and A.Y. Badretdinov, *A folding pathway solving Levinthal's paradox*, Prog. Biophys. Mol. Biol. 65 (1996), pp. 53–53.
[13] A. Sali, E. Shakhnovich, and M. Karplus, *How does a protein fold*, Nature 369 (1994), pp. 248–251.
[14] M.J. Buehler, and S. Keten, *Strength and resilience: A comparative study on mechanical signatures of alpha-helix, beta-sheet and tropocollagen domains*, Nano Res. 1 (2008), pp. 63–71.
[15] M.J. Buehler, *Tu(r)ning weakness to strength*, Nano Today 5 (2010), pp. 379–383.
[16] S.J. Stuart, A.B. Tutein, and J.A. Harrison, *A reactive potential for hydrocarbons with intermolecular interactions*, J. Chem. Phys. 112 (2000), pp. 6472–6486.
[17] D.W. Brenner, O.A. Shenderova, J.A. Harrison, S.J. Stuart, B. Ni, and S.B. Sinnott, *A second-generation reactive empirical bond order (REBO) potential energy expression for hydrocarbons*, J. Phys.-Condens. Matter. 14 (2002), pp. 783–802.
[18] A.D. MacKerell, D. Bashford, M. Bellott, R.L. Dunbrack, J.D. Evanseck, M.J. Field, S. Fischer, J. Gao, H. Guo, S. Ha, D. Joseph-McCarthy, L. Kuchnir, K. Kuczera, F.T.K. Lau, C. Mattos, S. Michnick, T. Ngo, D.T. Nguyen, B. Prodhom, W.E. Reiher, B. Roux, M. Schlenkrich, J.C. Smith, R. Stote, J. Straub, M. Watanabe, J. Wiorkiewicz-Kuczera, D. Yin, and M. Karplus, *All-atom empirical potential for molecular modeling and dynamics studies of proteins*, J. Phys. Chem. B 102 (1998), pp. 3586–3616.
[19] Q.B. Zheng, Y. Geng, S.J. Wang, Z.G. Li, and J.K. Kim, *Effects of functional groups on the mechanical and wrinkling properties of graphene sheets*, Carbon 48 (2010), pp. 4315–4322.
[20] A.F. Fonseca, G. Lee, T.L. Borders, H.J. Zhang, T.W. Kemper, T.R. Shan, S.B. Sinnott, and K. Cho, *Reparameterization of the REBO–CHO potential for graphene oxide molecular dynamics simulations*, Phys. Rev. B 84 (2011), 075460.
[21] S. Keten, Z.P. Xu, B. Ihle, and M.J. Buehler, *Nanoconfinement controls stiffness, strength and mechanical toughness of beta-sheet crystals in silk*, Nat. Mater. 9 (2010), pp. 359–367.
[22] Z. Qin and M.J. Buehler, *Molecular dynamics simulation of the alpha-helix to beta-sheet transition in coiled protein filaments: Evidence for a critical filament length scale*, Phys. Rev. Lett. 104 (2010), 198304.
[23] Z. Qin, L. Kreplak, and M.J. Buehler, *Hierarchical structure controls nanomechanical properties of vimentin intermediate filaments*, PLoS ONE 4 (2009), e7294.
[24] Z.P. Xu, and M.J. Buehler, *Geometry controls conformation of graphene sheets: Membranes, ribbons, and scrolls*, ACS Nano 4 (2010), pp. 3869–3876.
[25] F. Grater, P. Heider, R. Zangi, and B.J. Berne, *Dissecting entropic coiling and poor solvent effects in protein collapse*, J. Am. Chem. Soc. 130 (2008), pp. 11578–11579.
[26] J.F. Marko, and E.D. Siggia, *Stretching DNA*, Macromolecules 28 (1995), pp. 8759–8770.
[27] S. Park, and R.S. Ruoff, *Chemical methods for the production of graphenes*, Nat. Nanotech. 4 (2009), pp. 217–224.
[28] S. Keten, and M.J. Buehler, *Geometric confinement governs the rupture strength of H-bond assemblies at a critical length scale*, Nano Lett. 8 (2008), pp. 743–748.
[29] Z. Qin, and M.J. Buehler, *Cooperative deformation of hydrogen bonds in beta-strands and beta-sheet nanocrystals*, Phys. Rev. E 82 (2010), 061906.
[30] M.J. Buehler, *Strength in numbers*, Nat. Nanotech. 5 (2010), pp. 172–174.